Electrosynthesis of SER-Active Silver Nanopillar Electrode Arrays[†]

Jiu-Ju Feng,[‡,⊥] Ya-Hui Lu,[⊥] Ulrich Gernert,[§] Peter Hildebrandt,[‡] and Daniel H. Murgida*[,∥]

Institut für Chemie, Technische Universität Berlin, Sekr. PC14, Straβe des 17. Juni 135, D-10623-Berlin, Germany, Zentraleinrichtung Elektronenmikroskopie, Technische Universität Berlin, Strasse des 17. Juni 135, D-10623 Berlin, Germany, Departamento de Química Inorgánica, Analítica y Química Física/ INQUIMAE-CONICET, Facultad de Ciencias Exactas y Naturales, Universidad de Buenos Aires, Ciudad Universitaria, Pab. 2, piso 1, C1428EHA Buenos Aires, Argentina, and School of Chemistry and Environmental Science, Henan Normal University, Xinxiang, Henan 453007, China

Received: September 1, 2009; Revised Manuscript Received: December 15, 2009

Here we report a one step electrochemical method for the deposition of pillar-like silver nanostructures on graphite plate electrodes. The devices were tested as SER-active electrode arrays using covalently attached hemin. The nanopillar arrays provide reproducible surface enhanced resonance Raman (SERR) signals within 6% standard deviation and Raman enhancement factors of 1×10^5. They also show good electrochemical performance, as verified by potential-dependent SERR spectroscopy and cyclic voltammetry. Furthermore, the hemin-coated arrays display mediatorless electrocatalytic activity toward NO_2^-. Thus, the Ag nanopillar arrays present good prospects for their application in sensing devices and for SER/SERR based spectroelectrochemical applications in general.

Introduction

Surface-enhanced Raman (SER) spectroscopy has been early recognized as a convenient and sensitive technique for investigating surface adsorbates. Since the discovery of the SER effect by Fleischmann et al.[1] about 35 years ago, significant progress has been made in terms of instrumentation and SER-active substrates, such that nowadays it can be regarded as a well established analytical tool in several fields of chemistry, material science and biophysics.[2−19] So far two distinct enhancement mechanisms have been identified. The chemical mechanism, on one hand, is based on charge transfer interactions between the substrate and the adsorbate and provides a weak enhancement solely for molecules in direct contact to the metal.[20] The electromagnetic mechanism (EM), on the other hand, is based on the amplified electromagnetic fields generated upon excitation of the localized surface plasmons of nanostructured metals.[21,22] This latter mechanism does not require specific substrate/adsorbate contacts as the electromagnetic fields of the surface plasmons decay exponentially and is responsible for most of the enhancement observed experimentally. Among the different metals tested as SER substrates Ag presents the strongest EM enhancements, giving rise to intense surface plasmon absorption in the visible wavelength range. A drawback, however, is that Ag nanostructures are less stable and inert than their Au counterparts. In addition, the low oxidation potential of Ag imposes a more limited potential window for SER-based spectro-electrochemical applications. For these reasons most efforts in recent years have been devoted to the development of Au SER substrates, including SER-active electrodes,[7,11,12,23−25] although the attractiveness of the unsurpassed Ag sensitivity has also driven significant efforts with this metal and with hybrid Ag/Au structures.[7,11,12,23,26,27] To this end, a large number of highly regular and reproducible Au and Ag SER substrates have been reported, making use of spheres, tubes, rods, thorns, cavities, wires, etc., as building blocks.

The utilization of Ag as SER-active substrate is particularly suited for the analysis of adsorbates such as porphyrins and heme proteins. The absorption spectra of these molecules present maxima at ca. 410 nm (Soret band) with extinction coefficients above 10^5 M^{-1} cm^{-1}. Thus, by proper choice of the laser line, it is possible to excite simultaneously the surface plasmons of Ag nanostructures and the electronic transitions of the adsorbate, thereby combining the intensification provided by the molecular resonance Raman (RR) and SER effects (SERR).[13,18]

For quantitative spectro-electrochemical applications the substrates must fulfill several requirements: (i) the Raman enhancement factors need to be high and reproducible, (ii) the nanostructured surface should have a good electrochemical performance, (iii) the active area should be sufficiently high to allow for a high load of the analyte, and (iv) the preparation procedure of the SER-active substrates should be simple and inexpensive for routine applications.

Here we report a very simple one-step procedure for obtaining arrays of Ag nanopillar structures. The method is based on the electrodeposition of the metal on graphite electrodes using SDS and NH_4^+ ions as structure directing agents. The resulting structures are characterized in terms of their SER performance and as nanoelectrode arrays using covalently attached hemin as SERR and redox probe.

Materials and Methods

Reagents. Hemin, *N*-succinimidyl-3-maleimidopropionate, sodium dodecyl sulfate (SDS), and cystamine (2,2′-diaminodiethyl disulfide) were obtained from Sigma-Aldrich and used without further purification. All other chemicals were of analytical grade. Phosphate buffer solutions (PBS, pH 7.0) were prepared by mixing 12.5 mM solutions of K_2SO_4, Na_2HPO_4,

[†] Part of the "Martin Moskovits Festschrift".

* Corresponding author. E-mail: dhmurgida@qi.fcen.uba.ar.
[‡] Institut für Chemie, Technische Universität Berlin.
[§] Zentraleinrichtung Elektronenmikroskopie, Technische Universität Berlin.
[∥] Universidad de Buenos Aires.
[⊥] Henan Normal University.

10.1021/jp9084469
Published on Web 01/08/2010

and NaH_2PO_4. All the solutions were prepared with deionized water ($R > 18$ MΩ).

Characterization. The Ag deposits were characterized by scanning electron microscopy (SEM) with a Hitachi S-4000 field emission scanning electron microscope, and by X-ray diffraction (XRD) with a Philips PW 1830 diffractometer, using a monochromatized X-ray beam with nickel-filtered Cu Kα radiation.

Spectroscopic and Electrochemical Studies. SERR spectra were collected at ambient temperature using 413 nm excitation (2.5 mW at the sample) from a continuous wave (cw) krypton ion laser (Coherent Innova 300) and a confocal Raman microscope (LabRam HR-800, Jobin Yvon) equipped with a liquid-nitrogen-cooled CCD detector. The laser beam was focused on the surface of a disk carbon electrode by means of a long working distance objective (20×; N.A. 0.35). All spectra shown in this paper are normalized to the power of 2.5 mW and accumulation time of 20 s. Spectra were measured with a resolution of 2 cm^{-1} and an increment per data point of 0.57 cm^{-1}. RR spectra of hemin in solution (50 μM) were measured under the same scattering geometry using 3 mW laser power and an accumulation time of 100 s. For comparison, the RR intensities were normalized as in the case of the SERR experiments.

The carbon working electrode was placed in a home-built electrochemical cell, which includes a Pt wire and an Ag/AgCl (saturated KCl) electrode as a counter and reference electrodes, respectively. The exposed area of the working electrode was controlled by a Viton O-ring and determined to be 0.90 cm^2. For SERR experiments the cell was mounted on an eccentrically rotating device such that the electrode surface is continuously moved with respect to the laser beam. Electrode potentials were controlled with a PAR263A potentiostat (Princeton Applied Research). Additionally, electrochemical measurements were performed with the same cell using a CH Instrument Electrochemical Analyzer 618B. All potentials cited in this work refer to the Ag/AgCl (saturated KCl) reference electrode.

Preparation of Ag Nanopillar Arrays. The graphite working electrodes were polished following standard procedures. Electrodeposition of Ag nanopillar arrays was carried out potentiostatically at various potentials for 300 s in solutions (20 mL) containing 0.02 g of $AgCH_3COO$, 0.04 g of SDS, 0.2 mL of NH_3(aq), 0.2 g of NH_4CH_3COO, and 0.1 M KNO_3, at room temperature. SDS was removed from the electrode surface by thorough washing with ethanol and water. After drying under nitrogen stream at room temperature, the Ag nanopillar arrays were immersed into a 50 mM cysteamine solution overnight to form a self-assembled monolayer. The cysteamine-coated arrays were treated with 1.0 mM *N*-succinimidyl-3-maleimidopropionate in HEPES for 2 h, followed by rinsing with HEPES and water. The maleimide-coated arrays were placed in a solution containing 50 μM hemin in HEPES solution (pH 7.5) for 2 h, and then rinsed with water.

Results and Discussion

Silver nanostructures were grown on carbon disk electrodes by electrodeposition from Ag^+/NH_4^+ solutions containing SDS as structure-directing agent. Figure 1 shows SEM micrographs (top view and cross section) of the structures obtained at a deposition potential of −600 mV. Under these conditions the Ag deposit has the appearance of a dense array of pillar-like nanostructures (about 140 pillars/μm^2) with average dimensions of 90 ± 15 nm in diameter, 400 ± 25 nm height, and about 60 ± 10 nm distance between two adjacent nanopillars.

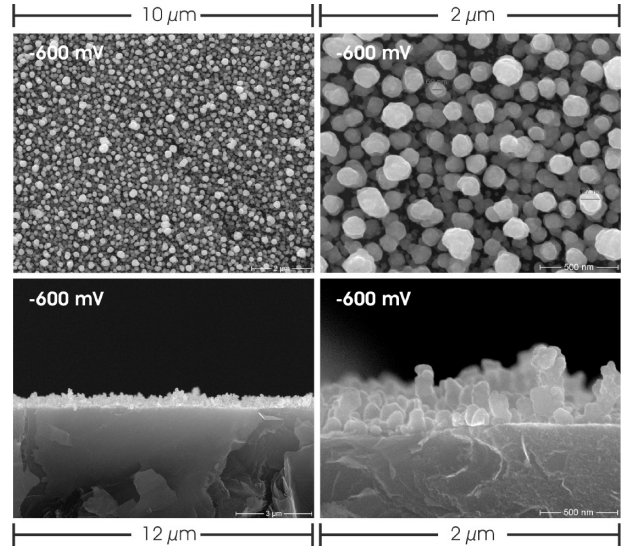

Figure 1. SEM images of Ag nanostructures electrodeposited on a carbon graphite plate at −600 mV for 300 s. Top: top views. Bottom: cross sections.

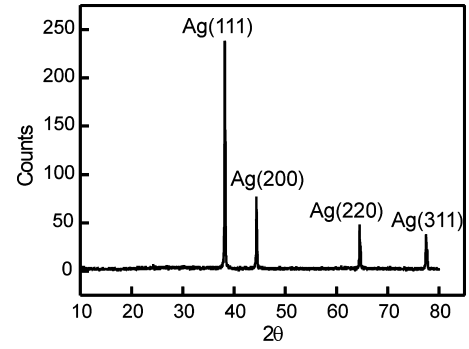

Figure 2. XRD pattern of an Ag nanopillar array prepared as described in Figure 1.

XRD patterns collected from the nanopillar arrays display the characteristic peaks of crystalline Ag with (111), (200), (220), and (311) facets (Figure 2).

The morphology of the Ag deposit is strongly dependent on the deposition potential. For potentials above −100 mV no nanopillar structures are formed and, instead, only a few Ag particles of about 1.2 μm in diameter are observed decorating the carbon plate (Figure 3). As the deposition potential is lowered, the coverage increases yielding dendritic structures, which start to resemble nanopillar structures at ca. −400 mV to finally yield relatively well-defined and reproducible nanopillar arrays within the range from −500 to −600 mV (Figure 1). Further lowering of the deposition potential leads to porous unordered structures, as shown in Figure 3.

Surfactants such as SDS are known to adsorb on electrodes affecting the kinetics of heterogeneous electron transfer, thereby directing crystal grow during the electrodeposition process.[28] Indeed, SDS and other surfactants have been used as a soft templates for the electrosynthesis of nanostructured films of a wide range of materials, including metals and metal oxides.[27−35] However, Ag deposition from SDS-containing solutions does not produce nanopillar structures in the absence of NH_4^+.[27] Conversely, no nanopillar structures are formed in the absence of SDS. Under the present experimental conditions Ag^+ access to the electrode surface is controlled by diffusion through complexation of Ag^+ and NH_4^+ by SDS. Nucleation and lateral/perpendicular growth of the Ag nanopillar structures strongly

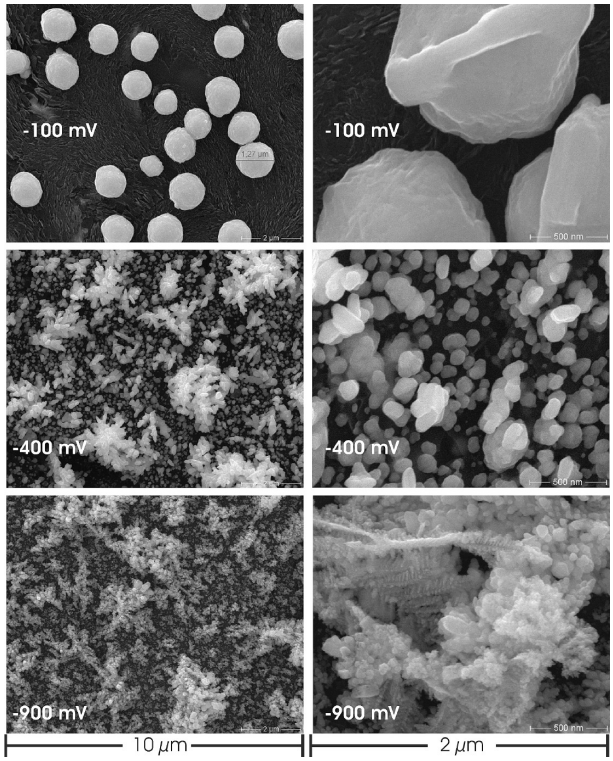

Figure 3. SEM images of Ag nanostructures electrodeposited on a carbon graphite plate at various potentials for 300 s.

depends on the deposition potential, which in turn controls the density and diameter of nanopillars.

To determine the optical absorbance, the Ag nanostructures were prepared on indium tin oxides substrates at different deposition potentials. The spectra do not display pronounced absorption maxima but an absorbance in the entire spectral window from 400 to 800 nm. The magnitude of the absorbance, however, sensitively depends on the deposition potentials at which the nanostructures are formed (Supporting Information, Figure S1). The strongest absorbance is observed for −500 mV (i.e., under conditions where the largest amount of Ag is deposited on the electrode surface). In this case, even at 800 nm an appreciable absorbance is noted. The overall absorbance was lower for −900 mV as well as for more positive potentials (−400 and −100 mV).

In order to test the performance of the Ag deposits as SER-active electrode arrays, preparations obtained at different electrodeposition potentials were coated with self-assembled monolayers of cysteamine to which hemin was subsequently cross-linked to obtain a surface-confined redox active SER probe. Figure 4A shows SERR spectra recorded for the ferrous form of hemin immobilized on Ag deposits obtained at various electrodeposition potentials. In all cases, the recorded SERR spectra display the characteristic features of fully reduced hemin and display excellent signal-to-noise ratios. However, the absolute intensity shows a clear correlation with the electrodeposition potential, with a maximum at −500 mV. Note that this deposition potential corresponds to the formation of regular nanopillar arrays as inferred from the SEM micrographs (vide supra).

Vibrational modes observed in the marker band region (ca. 1250−1750 cm^{-1}) of Raman spectra of porphyrins are largely dominated by modes including C−C and C−N stretching vibrations. Due to the increased electron back-donation of Fe^{2+} compared to Fe^{3+} into the π^* orbital of the porphyrin, which

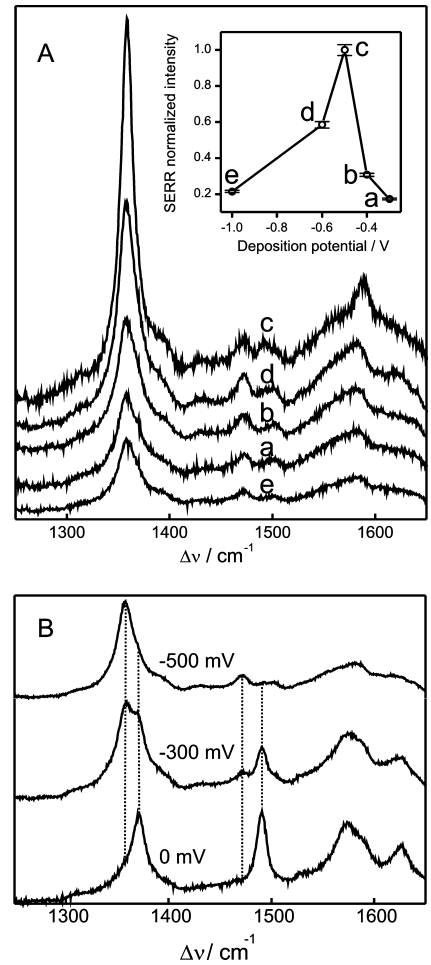

Figure 4. (A) SERR spectra of ferrous hemin covalently attached to Ag structures obtained by electrodeposition at different potentials. The inset shows normalized SERR intensities as a function of the electrodeposition potential. (B) SERR spectra of hemin covalently attached to Ag nanopillar as a function of the applied potential. The electrodeposition potential for this preparation was −500 mV.

weakens the C−N bonds, most bands are significantly up-shifted upon oxidation.[13,18,36] SERR spectra of the hemin-coated nanopillar preparations sensitively respond to the applied potential displaying reversible band shifts that indicate direct electronic communication of the immobilized redox probe with the carbon plate electrode through the Ag nanostructures (Figure 4B).

Direct electron transfer of hemin immobilized on SAM-coated nanopillar arrays was further confirmed by cyclic voltammetry. Typical voltammograms are shown in Figure 5A. The average formal redox potential from several preparations is about −350 ± 10 mV, which is very close to the value for hemin in solution.[37] Upon increasing the scan rate from 20 to 1000 mV s^{-1} peak currents increase linearly, as expected for surface confined species (Figure 5B). From the separation between the anodic and cathodic peaks as a function of the scan rate (Figure 5C), and using Laviron's formalism,[38] we estimate a standard electron transfer rate constant $k^\circ = 16\ s^{-1}$ for the immobilized hemin. This value is comparable to others reported for hemin modified electrodes, including pyrolytic graphite[39] and, thus, indicates a good electrochemical performance of the nanopillar arrays.

On the basis of the CV measurements, the actual surface area and hemin coverage were determined for the silver nanostructures obtained at different deposition potentials. For deposition potentials of −100, −400, −500, and −900 mV, the surface

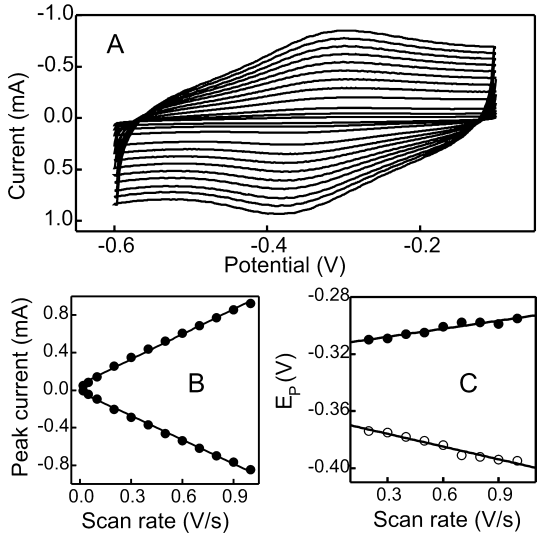

Figure 5. (A) Cyclic voltammograms of a hemin-coated nanopillar electrode array recorded at various scan rates between 20 and 1000 mV s^{-1}. (B) Scan rate dependence of the peak currents. (C) Peak positions as a function of the scan rate.

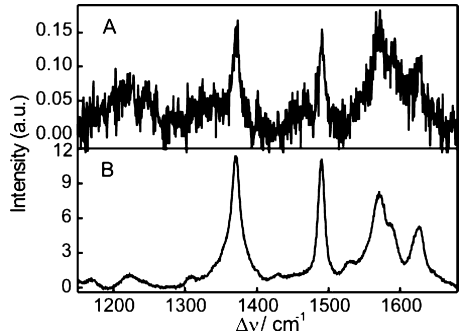

Figure 6. (A) RR spectrum of hemin in solution (50 μM) and (B) SERR spectrum of hemin covalently attached to an Ag nanopillar electrode. Both measurements were performed under otherwise identical conditions.

area was determined to be ca. 3.85, 4.58, 5.72, and 4.82 cm^2, respectively, whereas the average surface concentration of hemin was estimated to be 1.64×10^{-10}, 1.78×10^{-10}, 3.19×10^{-10}, and 0.97×10^{-10} mol cm^{-2}, respectively. Thus, the active surface area was between 4 and 6 times larger than the geometric area of the graphite support (0.90 cm^2).

The surface enhancement factor of the nanopillar arrays electrodeposited at −500 mV was estimated by comparison of SERR spectra of covalently attached hemin and RR spectra of the same compound in solution (Figure 6). Since in the confocal setup the determination of the number of molecules in the solution contributing to the detected RR intensity is associated with substantial errors,[40] we have chosen cytochrome *c* (Cyt-c) as a reference system. For Cyt-c adsorbed on colloidal silver particles the enhancement factor at 407 nm excitation has been determined to be 8×10^4.[41] Assuming that the enhancement is the same for electrochemically roughened silver electrodes at 413 nm excitation, we may estimate the enhancement factor EF_{Cyt} for Cyt-c immobilized on an electrochemically roughened silver electrode coated with a self-assembled monolayer (SAM) of mercaptounodecanoic acid by taking into account the distance-dependent drop of the enhancement by a factor of 2.5 (i.e., $EF_{Cyt} = 3.2 \times 10^4$).

Both the Cyt-c/SAM/Ag and the hemin/nanopillar/graphite device, on one hand, and Cyt-c and hemin solutions, on the other hand, can now be measured under identical conditions. Normalizing the respective SERR and RR intensities ($I_{SERR,Hem}$, $I_{SERR,Cyt}$, $I_{RR,Hem}$, and $I_{RR,Cyt}$) to the same accumulation time and laser power, the enhancement factor of hemin on silver nanopillar arrays (EF_{Hem}) with respect to hemin in solution can now be determined without knowing the probe volume in the solution experiment. Then one obtains

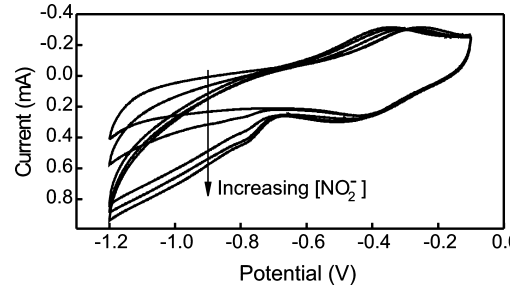

Figure 7. Cyclic voltammograms of a hemin-coated nanopillar electrode array recorded in the presence of variable amounts of NO_2^-.

$$EF_{Hem} = EF_{Cyt}\frac{I_{SERR,Hem}I_{RR,Cyt}}{I_{SERR,Cyt}I_{RR,Hem}}\frac{c_{Ag,Cyt}}{c_{Nano,Hem}}\frac{c_{Sol,Hem}}{c_{Sol,Cyt}} \quad (1)$$

where $c_{Sol,Cyt}$ and $c_{Sol,Hem}$ denote the bulk concentration in the solution experiments of Cyt-c and hemin, respectively. The surface concentration of Cyt-c and hemin ($c_{Ag,Cyt}$ and $c_{Nano,Hem}$) refers to the number of adsorbed molecules in the focus of the laser. For $c_{Ag,Cyt}$ we take the value for the surface coverage previously determined for Cyt-c on SAM-coated silver electrodes and the corresponding quantity for hemin is given by the surface coverage and the effective surface area of the nanopillar array prepared at −500 mV. Then EF_{Hem} is determined to be 1×10^5. This value is even slightly higher than that determined for Cyt-c on colloidal silver (8×10^4) and thus most likely distinctly higher than for hemin on silver colloids since Cyt-c has been shown to exhibit an intrinsically stronger enhancement than hemin.[41]

The intensity of the SERR spectra of hemin drops substantially when using deposition potentials that are higher or lower than −500 mV. However, taking into account the surface area and surface coverage, the decrease of the enhancement factor is moderate with 9×10^4 and 7×10^4 for deposition potentials of −900 and −400 mV, respectively. Thus, silver nanopillar structures prepared at −500 mV provide excellent SERR signals partly due to the high surface area and partly due to the specific optical properties as reflected by the absorption spectra (vide supra). Furthermore, the intensity of the SERR signal determined from several different nanopillar/hemin preparations was reproducible within 6% standard deviation which is distinctly better than for electrochemically roughened silver electrodes (>15%).

As a proof of principle, the nanopillar/hemin electrodes were tested as NO_2^- amperometric sensors. Upon addition of NO_2^- to a buffered solution (pH 7.0, potassium phosphate) we observe a new reduction peak that increases with the concentration of NO_2^- (Figure 7). This peak is ascribed to the hemin/nitrosyl adduct.[42] Direct reduction of NO_2^- was not observed at the bare electrode arrays. Upon inserting the nanopillar electrodes into NO_2^- containing solutions the reduction currents measured at −895 mV increase steeply within 3 s to reach stable values.

The response is linear for NO_2^- concentrations from 10 μM to 0.5 mM, with a detection limit of 1.2 μM at signal-to-noise ratio of 3.

Conclusions

Nanopillar arrays were grown on graphite disk electrodes by diffusion-limited electrodeposition of Ag using SDS and NH_4^+ as structure-directing agents. At the optimal deposition potential of ca. −500 mV, the nanopillar structures are highly regular and reproducible with average dimensions of 90 ± 15 nm in diameter, 400 ± 25 nm in height, and 60 ± 10 nm separation between adjacent nanopillars. Using hemin covalently attached to the Ag structures, it is shown that the arrays provide excellent and reproducible Raman enhancement, as well as good performance as electrodes. Furthermore, the hemin-coated arrays show good mediatorless electrocatalytic activity toward NO_2^-, thereby presenting good prospects for its application in sensing devices.

In summary, we have developed a simple and inexpensive method for growing reproducible SER-active nanoelectrode arrays that can be of great utility in combined SER/SERR-electrochemical studies with basic and applied purposes.

Acknowledgment. Financial support from ANPCyT (PICT2006-459) to D.H.M., the Sfb448 (P.H.), the Cluster of Excellence Unicat, and the National Science Foundation of China (J.J.F.; NSFC No. 20905021) are gratefully acknowledged.

Supporting Information Available: Absorption spectra of Ag nanopillar structures. This material is available free of charge via the Internet at http://pubs.acs.org.

References and Notes

(1) Fleischmann, M.; Hendra, P. J.; Mcquillan, A. J. *Chem. Phys. Lett.* **1974**, *26*, 163.
(2) Kneipp, K., Moskovits, M., Kneipp, H. E., Eds.; *Surface-Enhanced Raman Scattering. Physics and Applications*; Springer-Verlag: Berlin, 2006.
(3) Han, X. X.; Zhao, B.; Ozaki, Y. *Anal. Bioanal. Chem.* **2009**, *394*, 1719.
(4) Lombardi, J. R.; Birke, R. L. *Acc. Chem. Res.* **2009**, *42*, 734.
(5) Banares, M. A.; Mestl, G. *Adv. Catal.* **2009**, *52*, 43.
(6) Camden, J. P.; Dieringer, J. A.; Zhao, J.; Van Duyne, R. P. *Acc. Chem. Res.* **2008**, *41*, 1653.
(7) Brown, R. J. C.; Milton, M. J. T. *J. Raman Spectrosc.* **2008**, *39*, 1313.
(8) Kudelski, A. *Talanta* **2008**, *76*, 1.
(9) Tripp, R. A.; Dluhy, R. A.; Zhao, Y. P. *Nano Today* **2008**, *3*, 31.
(10) Chen, L. X.; Choo, J. B. *Electrophoresis* **2008**, *29*, 1815.
(11) Banholzer, M. J.; Millstone, J. E.; Qin, L. D.; Mirkin, C. A. *Chem. Soc. Rev.* **2008**, *37*, 885.
(12) Lal, S.; Grady, N. K.; Kundu, J.; Levin, C. S.; Lassiter, J. B.; Halas, N. J. *Chem. Soc. Rev.* **2008**, *37*, 898.
(13) Murgida, D. H.; Hildebrandt, P. *Chem. Soc. Rev.* **2008**, *37*, 937.
(14) Pieczonka, N. P. W.; Aroca, R. F. *Chem. Soc. Rev.* **2008**, *37*, 946.
(15) Porter, M. D.; Lipert, R. J.; Siperko, L. M.; Wang, G.; Narayanana, R. *Chem. Soc. Rev.* **2008**, *37*, 1001.
(16) Bell, S. E. J.; Sirimuthu, N. M. S. *Chem. Soc. Rev.* **2008**, *37*, 1012.
(17) Wu, D. Y.; Li, J. F.; Ren, B.; Tian, Z. Q. *Chem. Soc. Rev.* **2008**, *37*, 1025.
(18) Murgida, D. H.; Hildebrandt, P. *Acc. Chem. Res.* **2004**, *37*, 854.
(19) Kneipp, K.; Kneipp, H.; Itzkan, I.; Dasari, R. R.; Feld, M. S. *J. Phys. Cond. Matt.* **2002**, *14*, R597.
(20) Otto, A.; Futamata, M. *Top. Appl. Phys.* **2006**, *103*, 147.
(21) Moskovits, M. *Rev. Mod. Phys.* **1985**, *57*, 783.
(22) Moskovits, M.; Suh, J. S. *J. Phys. Chem.* **1984**, *88*, 5526.
(23) Lu, X. M.; Rycenga, M.; Skrabalak, S. E.; Wiley, B.; Xia, Y. N. *Annu. Rev. Phys. Chem.* **2009**, *60*, 167.
(24) Cole, R. M.; Mahajan, S.; Bartlett, P. N.; Baumberg, J. J. *Opt. Express* **2009**, *17*, 13298.
(25) Mahajan, S.; Baumberg, J. J.; Russell, A. E.; Bartlett, P. N. *Phys. Chem. Chem. Phys.* **2007**, *9*, 6016.
(26) Feng, J. J.; Gernert, U.; Sezer, M.; Kuhlmann, U.; Murgida, D. H.; David, C.; Richter, M.; Knorr, A.; Hildebrandt, P.; Weidinger, I. M. *Nano Lett.* **2009**, *9*, 298.
(27) Feng, J. J.; Hildebrandt, P.; Murgida, D. H. *Langmuir* **2008**, *24*, 1583.
(28) Gomes, A.; Pereira, M. I. D. *Electrochim. Acta* **2006**, *52*, 863.
(29) Chang, I. C.; Huang, T. K.; Lin, H. K.; Tzeng, Y. F.; Peng, C. W.; Pan, F. M.; Lee, C. Y.; Chiu, H. T. *ACS App. Mat. Int.* **2009**, *1*, 1375.
(30) Anandan, V.; Rao, Y. L.; Zhang, G. G. *Int. J. Nanomed.* **2006**, *1*, 73.
(31) Inamdar, A. I.; Mujawar, S. H.; Ganesan, V.; Patil, P. S. *Nanotech.* **2008**, *19*.
(32) Lin, Y. C.; Duh, J. G. *J. Alloys Compd.* **2007**, *439*, 74.
(33) Sato, H.; Homma, T.; Kudo, H.; Izumi, T.; Osaka, T.; Shoji, S. *J. Electroanal. Chem.* **2005**, *584*, 28.
(34) Liao, L. B.; Liu, W. H.; Xiao, X. M. *J. Electroanal. Chem.* **2004**, *566*, 341.
(35) Ghanem, M. A.; Bartlett, P. N.; de Groot, P.; Zhukov, A. *Electrochem. Commun.* **2004**, *6*, 447.
(36) Hu, S. Z.; Morris, I. K.; Singh, J. P.; Smith, K. M.; Spiro, T. G. *J. Am. Chem. Soc.* **1993**, *115*, 12446.
(37) Das, D. K.; Bhattaray, C.; Medhi, O. K. *J. Chem. Soc. Dalton* **1997**, 4713.
(38) Laviron, E. *J. Electroanal. Chem.* **1979**, *101*, 19.
(39) Chen, J.; Wollenberger, U.; Lisdat, F.; Ge, B. X.; Scheller, F. W. *Sensors Actuat. B Chem.* **2000**, *70*, 115.
(40) Baldwin, K. J.; Batchelder, D. N. *Appl. Spectrosc.* **2001**, *55*, 517.
(41) Hildebrandt, P.; Stockburger, M. *J. Phys. Chem.* **1986**, *90*, 6017.
(42) Feng, J. J.; Xu, J. J.; Chen, H. Y. *Electrochem. Commun.* **2006**, *8*, 77.

JP9084469